Lithium-ion Battery Life Cycle Prediction with Deep Learning Regression Model

Huawei Yang, Yuan Cao, Huaiqi Xie, Shuai Shao,
Jie Zhao, Tianyi Gao, Jiajun Zhang, Binghua Zhang
Baidu US Development Center
Sunnyvale, CA, USA
Email: huaweiyang@baidu.com

Abstract – **This paper presents a data-driven regression model to predict the life cycle of lithium-ion battery. The model is built based on five different key features derived from discharging voltage, current, time, and skin temperature. These sets of data are commonly available in most Battery Management Systems (BMS), which makes the proposed regression model widely applicable to various battery systems. The five-key-feature-based battery model is evaluated and validated all through the paper and is proved to have high prediction accuracy of battery life cycles. The proposed regression model can be utilized for real-time life cycle prediction without the need of historical data.**

Keywords—Lithium-ion battery, life cycle, state-of-heath, battery management system, real-time detection, deep learning regression

I. INTRODUCTION

Battery Energy Storage System (BESS) is widely used in a variety of applications, such as consumer electronics, electrical vehicles (EVs), uninterrupted power supply (UPS), data center, smart grid and medical devices [1-10], etc. Nowadays, lithium-ion battery is the most commonly used battery type in BESS.

However, because of the chemical nature of lithium-ion battery, the battery capacity or the ability to provide certain power decreases over the battery lifetime after many cycles of discharging and charging operation. In other words, the State of Health (SOH) of lithium-ion battery decreases with aging process. As a result, it is important and necessary to assess the battery aging state for safety and optimum operation. Once the health alarm reaches the preset limitation, the battery cell or battery module should be replaced from the battery system. Currently, there is no strict definition of SOH for lithium-ion battery. Remaining capacity, internal impedance and remaining life cycle of battery are the most commonly used indicators to reflect the energy and power capability [11-16].

The SOH detection and prediction of lithium-ion battery have been extensively studied with various methods, technologies and tools. Typically, the SOH detection method can be divided into two categories: experimental assessment method and data driven method (artificial intelligence method) [10-19]. Experimental methods utilize hardware equipment or test tools to detect related parameters to analyze the battery aging behavior. Coulomb counting (CC) method, open circuit voltage (OCV) method and Electrochemical impedance spectroscopy (EIS) method are commonly used. These methods are relatively simple and easy to implement. However, expensive hardware devices may be required.

Compared with experimental methods, some researchers consider SOH estimation issue as a black box. Even without prior knowledge about battery aging mechanism, Artificial Intelligence (AI) and machine learning methods can help estimate the SOH status. The AI-based methods can be further divided into two categories, the first one is adaptive model-based methods through mathematical derivation, such as Kalman filter, particle filter, least square and their enhanced/extended algorithms. The second category is data-driven methods, such as fuzzy logic, neural network, support vector machine and their enhanced/extended algorithms. Recently, the AI-based SOH estimation methods of lithium-ion battery are increasingly attracting attention.

In this paper, a data-driven regression model is utilized to predict the life cycle of lithium-ion battery. This method enables the model with real-time life cycle prediction based on one discharging cycle without the need of historical data. The structure of the rest paper is as follows: in Section II, detailed feature engineering and analysis of deep-learning regression model are provided. Following that, the model setup with dataset and prediction results are presented to evaluate and validate the proposed SOH model in Section III. The conclusion is given in Section IV.

978-1-7281-4829-8/20/$31.00 ©2020 IEEE

II. Feature Engineering and Deep Learning Regression Model

Five features are engineered from each discharging cycle based on the data of discharging voltage, discharging current, temperature and time.

A. DC Internal Resistance

Both International Electrotechnical Commission (IEC) and International Organization for Standardization (ISO) have standard DC Internal Resistance (DCIR) test procedures, which require certain controlled discharging current. However, in most commercially available applications, it is hard to achieve, measure and record a regulated discharging current. Therefore, an approximation method is required. Equation (1) shows a commonly used approximation method of DCIR assuming the capacity drop within a specified time interval is negligible such that the voltage drop is purely caused by DCIR, where V_{t1} and V_{t2} are the battery terminal voltage at time $t1$ and $t2$, respectively. I_{t2} is the discharging current at time $t2$.

$$DCIR = \frac{V_{t1} - V_{t2}}{I_{t2}} \tag{1}$$

B. Variance of Temperature

The skin temperature rises due to irreversible and reversible heat generation during battery discharging [9]. The irreversible heat is generated by I^2R while reversible heat is related to chemical reaction. With batteries degradation, the temperature rises further, which results in a higher variance. The variance of temperature per cycle is defined in (2), where T_i is the i^{th} temperature sample within each cycle and $Var(T_{cyc\_n})$ is the temperature variance of n^{th} cycle.

$$Var(T_{cyc\_n}) = E[(T_i - \mu)^2] \tag{2}$$

C. Variance of Discharging Voltage

Similarly, the discharging voltage turns to decrease faster towards to cutoff voltage while battery degrades. This also results in a higher variance. The variance of discharging voltage per cycle is defined in (3).

$$Var(V_{cyc\_n}) = E[(V_i - \mu)^2] \tag{3}$$

D. Discharge Capacity Difference Between First and Following Cycles

The discharge capacity difference between the first and following cycles, ΔQ_{1-n}, is directly proportional to battery degradation in a nonlinear relation in (4), where subscript n stands for the cycle number.

$$\Delta Q_{1-n} = Q_1 - Q_n \tag{4}$$

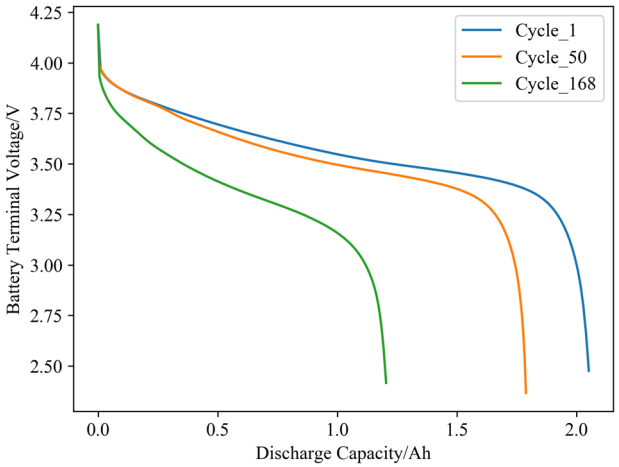

Fig. 1. Q-V curve of one example cell at different cycles

E. Variance of Discharging Voltage as a Function of Discharging Capacity

The Q-V curve of one sample cell at different cycles is shown in Fig. 1. It can be observed that the voltage difference at the same discharging capacity enlarges as life cycle increases. This indicates that a higher energy difference among different cycles is directly proportional to life cycle. Accumulated discharging capacity is calculated based on the instant discharging current at corresponding time, as described in (5), where Q_n is accumulated discharge capacity at the n^{th} sample and $(t_{i+1} - t_i)$ is the sampling time interval. Due to the sampling frequency and measurement resolution, as well as slight difference between each discharging cycle for the same cell, the discharging capacity at each sampling time is not consistent at different cycles. To standardize the Q-V data across cycles and cells, the sampled Q-V curve is fitted through a one-dimensional interpolating spline function. The increment of Q can be chosen at a reasonable rate for every corresponding voltage based on different cases. This uniform distribution enables the subtraction between voltages at the same capacity that is defined in (6), where ΔV_{n-m} is the

voltage difference between cycle n and m. V is a spline function of Q.

Fig. 2 shows an example of fitted Q-V curve as a comparison to the original Q-V curve in Fig. 1. The spline function is in good agreement with the original data.

$$Q_n = \sum_{i=1}^{n} I_i(t_{i+1} - t_i) \tag{5}$$

$$\Delta V_{n-m} = V_{cyc\_n}(Q) - V_{cyc\_m}(Q)$$
$$s.t. \quad V = S(Q) \tag{6}$$

Once ΔV is achieved, the variance of ΔV, as the proposed feature can be calculated similarly as previous variances in (7). Different from the definition of ΔQ as a function of discharge voltage in [12], in this paper, discharge voltage is defined as a function of ΔQ. This is because the capacity variation actually caused the voltage variation during both charging and discharging cycles. In addition, voltage deviates much more significantly at different cycles when compared to capacity change, as can be seen from Fig. 1.

$$Var(\Delta V_{n-m}) = E[(\Delta V_i - \mu)^2] \tag{7}$$

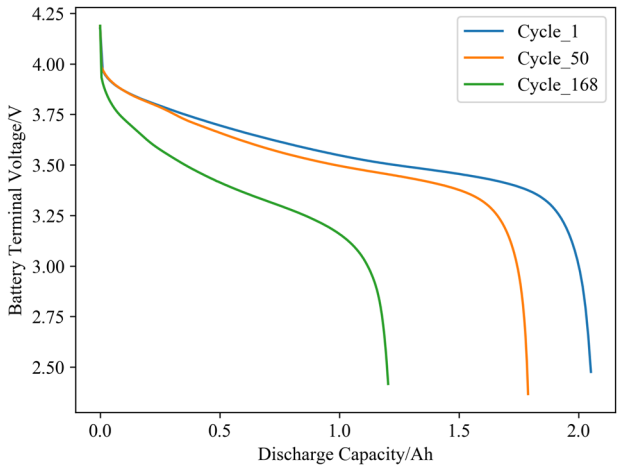

Fig. 2. Spline Fitted Q-V curve of the same example cell in Fig.1 at different cycles

F. Deep Learning Regression Model

Because all the engineered features are positively correlated to life cycle and the target model output is the predicted life cycle, regression model comes in place naturally. Compared to traditional regression model, such as linear or logistic regression, deep learning regression has higher complexity that can extract higher order correlations between features in this case. To use deep learning model as regression, the output layer will only have one neuron with linear activation and loss function of Mean Absolute Error (MAE) or Mean Square Error (MSE). The input layer and hidden layers can be configured according to specific datasets [20].

One of the disadvantages of deep learning regression model is the complexity compared with conventional statistical regression model. Deep learning regression usually consists multiple layers with thousands of parameters in total, which may lead to longer computing time. However, with only five engineered features proposed in this paper that are highly correlated to life cycle, the complexity caused by computing time can be negligible.

III. Model Setup and Results

A. Battery Dataset

Life cycle experiment test result of four Lithium-ion cells with rated capacity at 2Ah from [15] was used as the model training and prediction dataset. All cells were tested through charging, discharging, and impedance cycles at 23C. All cells were first charged at Constant Current (CC) mode at 1.5A to 4.2V and then switched to Constant Voltage (CV) mode. The cutoff charging current was set at 20 mA. The discharging cycles were performed at constant current of 2A. The discharging cutoff voltage varies in different cells. The test was stopped when the cell capacity reached below 1.4 Ah. However, the initial capacity varies and some of them were already below the rated 2Ah at the start. This characteristic gives the opportunity to test robustness of the model with cells at various condition. Detailed experiment parameters are listed in Table I. Initial capacity is calculated as in (5) at the first cycle. The capacity dropped below 80% after 75, 65, 98, and 60 cycles for cell 1~4 respectively.

TABLE I. Experiment Parameters

Cell Number	Charge Mode	Discharge Current (A)	Discharge cutoff voltage (V)	Initial Capacity (Ah)	Test End Cycle
Cell 1	1.5A CC, 4.2V CV, 20 mA cutoff	2.0	2.7	1.86	168
Cell 2			2.5	2.05	168
Cell 3			2.2	1.92	168
Cell 4			2.5	1.87	132

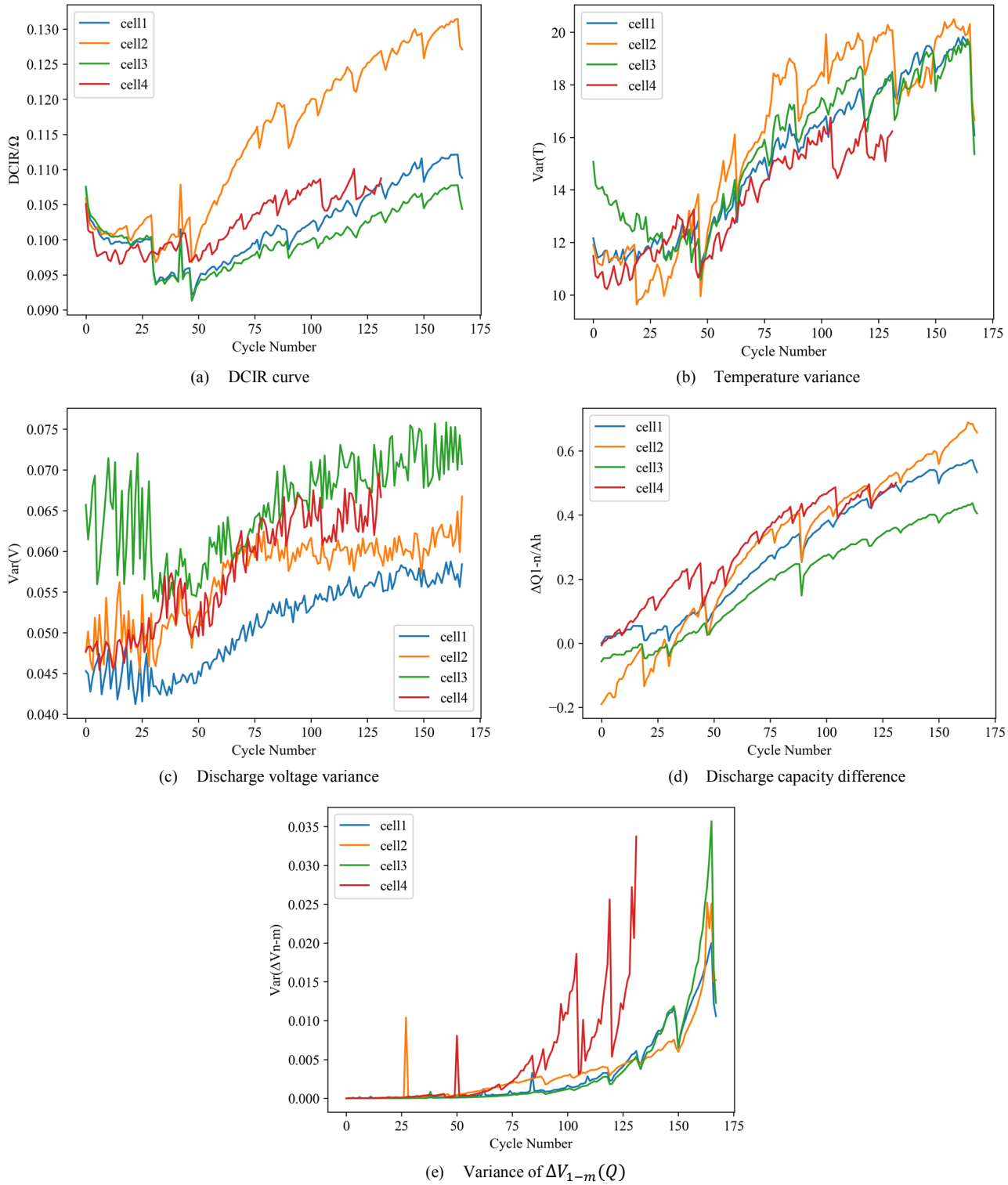

(a) DCIR curve

(b) Temperature variance

(c) Discharge voltage variance

(d) Discharge capacity difference

(e) Variance of $\Delta V_{1-m}(Q)$

Fig. 3. Five engineered features of four cells in the dataset

As introduced in Section II, five engineered features are calculated based on the raw discharging data of battery terminal voltage, output current, sampling time, and skin temperature. Feature $Var(\Delta V_{n-m})$ is set as $Var(\Delta V_{1-m})$, where

m ranges from second to the last test cycle in this dataset. Their relation is summarized in Table II.

Fig. 3 shows the correlation of five features to life cycle for all four cells. It can be clearly observed that all five features are positively correlated to life cycle, while cell 4 is slightly off to the other three due to early end life.

TABLE II. Feature and Discharging Data Relation

Engineered Feature	Related Raw Discharging Data			
	Terminal Voltage (V)	Output Current (A)	Skin Temperature (C)	Time (sec)
$DCIR$	✓	✓		
$Var(T)$			✓	
$Var(V)$	✓			
ΔQ_{1-n}		✓		✓
$Var(\Delta V_{n-m})$	✓	✓		✓

B. *Model Setup*

Five features are calculated at each cycle for all four cells. The features from cell 2 are selected as the training set because it has the full rated capacity initially compared with other cells. The other three cells are in test set. All features are normalized. This dataset setup allows the model to be trained with a typical cell under the regular condition while tested with cells at various conditions that meets the realistic battery working scenarios.

The deep learning regression model is constructed with Keras sequential model [20]. All layers are densely connected. The input layer has 64 nodes with 384 parameters. Only one hidden layer is added with 64 nodes to reduce the complexity. Both input and hidden layers are activated with Rectified Linear Unit (ReLU) [21]. The output layer has one node with linear activation for regression purpose.

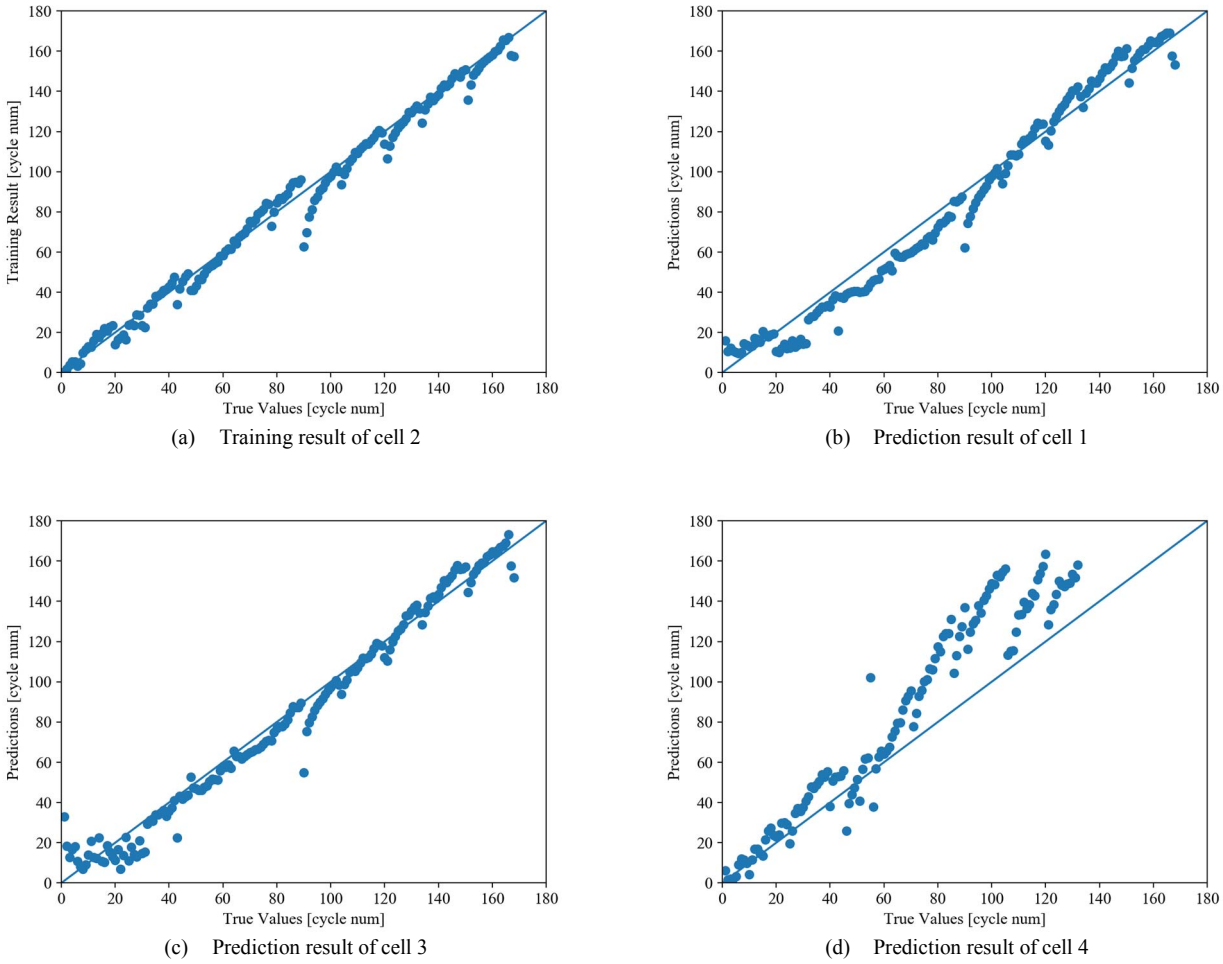

(a) Training result of cell 2

(b) Prediction result of cell 1

(c) Prediction result of cell 3

(d) Prediction result of cell 4

Fig. 4. Training and Prediction results

C. Training Environment and Prediction Results

The model is trained on a 2017 MacBook Pro with 2.8GHz i7 CPU and 16GB DDR3 RAM. It takes ~3 seconds with ~200 epochs to reach stable with early stopping. The training MAE is 4 cycles and MSE is 27. The prediction MAE of cell 1, 3 and 4 are 7, 5, and 18 cycles respectively. Fig. 4 depicts the training and prediction result of all four cells.

The prediction result indicates high linearity to the true life cycle number with reasonable low errors. Even the calculated capacity based on coulomb counting fades below 80% rated capacity much earlier than the end cycle of the experiment test for all cells, the model still provides high predication accuracy thanks to the highly correlated features. For cell 1 and 3, the prediction is a bit off during early cycles (<20 cycles). Possible reason is the initial conditions are different. For cell 4, the model predicts much higher life cycle after 70 cycles actually indicate high prediction accuracy because of the extensive degradation on cell 4. With only 132 total test cycles, the aging condition is at the same level as the other three if judged by capacity degradation. The life cycle prediction of cell 4 near the end of test is actually consist with other three, towards 150 ~ 160 cycles. It is also worth noting that for cell 1, 2, and 3, the value of all five features suddenly dropped at approximate 90 cycle, then increased again following the trend as of previous cycles. This behavior actually impacts the prediction result at the corresponding cycle, where the model predicted it to be ~60 cycle for all 3 cells while their true life cycle is around 90. This anomaly could be caused by data recording noises or imprecise measurements.

IV. Conclusion

This paper presents a deep learning regression model with five engineered features based on cell discharging voltage, current, temperature and time. The prediction result indicates high accuracy for cells under different aging conditions. All features can be achieved within one discharging cycle. This advantage enables building accurate life cycle prediction model without the need of historical data, which makes it more practical in real-world applications. The computation time is reasonable to achieve real-time prediction. This method is well suited in the scenarios where battery serves as energy storage or backup device, such as grid level energy storage and data centers.

References

[1] Y. Cao, H. W. Yang, T. Y. Gao, S. Shuai and B. H. Zhang, "Switched-mode Control of Battery Backup Unit in Data Center for Online Impedance Detection", *IEEE Application Power Electronics Conference (APEC)*, New Orleans, LA, March 2020.

[2] L. Chen, S.Wu, D. Shieh, and T. Chen, "Sinusoidal-ripple current charging strategy and optimal charging frequency study for li-ion atteries," *IEEE Trans. Ind. Electron.*, vol. 60, no. 1, pp. 88-97, Jan. 2013.

[3] Y. Cao and J. A. Abu Qahouq. "Evaluation of bi-directional single-inductor multi-input battery system with state-of-charge balancing control". IET Power Electronics, vol. 11, no. 13, pp. 2140-2150, Nov. 2018.

[4] Y. Yuanmao, K. W. E. Cheng, and Y. P. B. Yeung, "Zero-current switching switched-capacitor zero-voltage-gap automatic equalization system for series battery strings," *IEEE Trans. Power Electron*., vol. 27, no. 7, pp. 3234-3242, Jul. 2012.

[5] H. W. Yang, Y. B. Gao, K. B. Farley, M. Jerue, J. Perry and Z. Tse, "EV usage and city planning of charging station installations," *IEEE Wireless Power Transfer Conference (WPTC)*, May. 2015, pp. 1-4.

[6] J. A. Abu Qahouq and Y. Cao. "Control Scheme and Power Electronics Architecture for a Wirelessly Distributed and Enabled Battery Energy Storage System", *Energies* 2018, 11(7), 1887.

[7] Y. Li and Y. H. Han. "A module-integrated distributed battery energy storage and management system", *IEEE Trans. Power Electron*., vol. 31, no. 12, pp. 8260-8270, Dec. 2016.

[8] Y. Cao. "Small-signal Modeling and Analysis for Wirelessly Distributed and Enabled Battery Energy Storage System of Electrical Vehicles", *Applied Science* 2019, *9*(20), 4249

[9] C. Zhao, W. Cao, T. Dong, and F. Jiang, "Thermal behavior study of discharging / charging cylindrical lithium-ion battery module cooled by channeled liquid flow," *Int. J. Heat Mass Transf.*, vol. 120, pp. 751–762, 2018.

[10] W. Chwei-Sen, O. H. Stielau and G. A. Covic, "Design considerations for a contactless electric vehicle battery charger," *IEEE Transactions on Ind.Electron.,* vol. 52, no. 5, pp. 1308-1314, Oct. 2005.

[11] Y. Cao and J. A. Abu Qahouq. "Analysis and Evaluation of a Dual-Variable Closed-Loop Control of Power Converter with Wireless and Non-Wireless Power Transfer". *IEEE transaction on Industrial Electronics, vol*. 66, no. 4, pp. 2668-2679, Apr. 2019.

[12] K. A. Severson, P. M. Attia, N. Jin, N. Perkins, B. B. Jiang, Z. Yang, M. H. Chen, M. Aykol, P. K. Herring, D. Fraggedakis, M. Z. Bazant, S. J. Harris, W. C. Chueh, and R.D. Braatz. "Data-driven prediction of battery cycle life before capacity degradation", *Nature Energy*, vol. 4, no. 5, pp. 383-391.

[13] Y. Cao and J. A. Abu Qahouq. "Evaluation of Wireless Distributed and Enabled Battery Energy Storage System Under Unequal Battery Capacity Conditions", *IEEE Application Power Electronics Conference (APEC)*, Anaheim, CA, March 2019, pp. 1738-1742.

[14] Y. Cao and J. A. Abu Qahouq. "Evaluation of paralleled battery system with SOC balancing and battery impedance magnitude measurement", *IEEE Application Power Electronics Conference (APEC)*, San Antonio, Tx, March 2018, pp. 437-441.

[15] *Li-ion Battery Aging Datasets*, NASA Ames Research Center, Sep. 2010. [Online]. Available: https://c3.nasa.gov/dashlink/resources/133/, last access Nov. 2019.

[16] J. G. Zhu, Z. C. Sun, X. Z. Wei, and H. F. Dai, "A new lithium-ion battery internal temperature on-line estimate method based on electrochemical impedance spectroscopy measurement," *J. Power Sources*, vol. 274, pp. 990–1004, Jan. 2015.

[17] J. Kim, S. Lee, B. H. Cho, "Complementary cooperation algorithm based on DEKF combined with pattern recognition for SOC/capacity estimation and SOH prediction," *IEEE Trans. Power Electron*. vol. 27, no.1, pp. 436-451, Jan. 2012

[18] L. Ho-Ta, T. Liang, and S. M. Chen. "Estimation of battery state of health using probabilistic neural network." *IEEE Transactions on Industrial Informatics,* vol. 9, no. 2, pp. 436-451, 679-685, May 2013

[19] Nuhic, Adnan, et al. "Health diagnosis and remaining useful life prognostics of lithium-ion batteries using data-driven methods." *Journal of power sources* vol. 239, pp. 680-688, Oct, 2013.

[20] F. Chollet, "Keras.", (2015) Available: https://keras.io/, last access Nov. 2019.

[21] V. Nair, G. E. Hinton, "Rectified linear units improve restricted Boltzmann machines", International Conference on Machine Learning (ICML), Haifa, Israel, June 2010, pp. 807-814